Subsurface Transport Potential of Perfluoroalkyl Acids (PFAAs): Column Experiments and Modeling

Jennifer L. Guelfo[a,b,], Assaf Wunsch[b], John McCray[b], John F. Stults[b], Christopher P. Higgins[b,*]*

* Corresponding authors

[a]Department of Civil, Environmental, and Construction Engineering, Texas Tech University, Box 41023, Lubbock, TX 79409 USA

Email: jennifer.guelfo@ttu.edu

[b]Department of Civil and Environmental Engineering, 1500 Illinois St, Colorado School of Mines, Golden CO 80401 USA

Email: chiggins@mines.edu

ABSTRACT

Transport of ten perfluoroalkyl acids (PFAAs) was studied with one-dimensional (1-D) saturated column experiments using four soil types with an organic carbon fraction (f_{oc}) range of ~0-0.045. Columns were operated under conditions relevant to aqueous film-forming foam (AFFF)-impacted fire protection training areas to determine the ability of equilibrium transport parameters to describe 1-D PFAA transport, if rate-limited sorption influences PFAA transport, and if kinetic parameters can be used to evaluate factors causing rate-limited sorption. Results of initial screening of PFAA breakthrough found that over half of the breakthrough curves deviated from equilibrium transport and merited further investigation. Subsequent analysis showed that, in many cases, these deviations could be accounted for by considering the range of applicable equilibrium K_d values (i.e. based on standard

deviation) applicable to the solid phase. Thus, transport of the majority of PFAAs in 3 soils with f_{oc} of 0-0.017 was not impacted by rate-limited sorption. Further, low sorption led to transport that was essentially simultaneous for the majority of PFAAs in these porous media. Exceptions were observed for long-chain PFAAs, and also in a fourth soil with f_{oc} of 0.045, which indicated the potential for rate-limited sorption to impact transport in some scenarios. Subsequent flow interruption experiments isolating kinetic behavior confirmed rate-limited sorption caused nonequilibrium transport. Linear free energy relationships (LFERs) developed in previous work to predict the inverse relationship between mass transfer coefficients (k) and sorption parameters (i.e., K_d) were used to estimate values of k for PFAAs in this study. Resulting k values were 10^{-3} to 10^{-8} h^{-1}, consistent with previously measured kinetic parameters for other polar and anionic compounds. Models incorporating estimated k values resulted in improved predictions of breakthrough observed in nonequilibrium scenarios (R^2 0.83-0.98), but k values will require further validation prior to broader application. This work illustrates rate-limited sorption considerations are needed to describe 1-D column saturated transport for some PFAAs and solid phases. At field scales, subsurface heterogeneity and PFAA precursor transformation may be equally or even more important in determining saturated PFAA transport, but kinetic parameters in this study may help to determine relative contributions of rate-limited sorption to overall transport.

1. INTRODUCTION

Poly- and perfluoroalkyl substances (PFASs) have been manufactured and used in a variety of industrial and consumer products and processes since the early 1960s, including fluoropolymer manufacturing, nonstick coatings and a special class of firefighting foam known as aqueous film-forming foam (AFFF).[1] Designed for fighting fuel fires, AFFF is often utilized by fire-fighting facilities, the hydrocarbon industry, and the military.[2] In May 2016, the Environmental Protection Agency (EPA) issued drinking water health advisories of 0.07 μg/L for the sum of two PFASs: perfluorooctanoic acid (PFOA) and perfluorooctane sulfonic acid (PFOS).[3,4] Such low advisories are driven by concerns regarding human health risks to the developing fetus along with potential links to cancer and toxicity in the liver and kidney.[3,4] Activities such as fluoropolymer manufacturing and repeat use of AFFF at fire protection training areas (FPTAs) have led to comparatively high occurrence of PFASs in groundwater at μg/L to mg/L levels, [5–9] underscoring the need for comprehensive understanding of transport of these compounds in subsurface systems.

AFFF formulations are complex, proprietary, and often include solvents and both fluorinated (i.e. PFASs) and hydrocarbon surfactants.[10,11] PFASs include perfluoroalkyl acids (PFAAs, e.g. PFOS, PFOA) distinguishable by a fully saturated fluorocarbon tail comprised of strong carbon-fluorine bonds. These bonds make PFAAs chemically stable and generally resistant to processes such as hydrolysis, photolysis, and oxidation, and they are therefore extremely persistent in the environment.[1,12–14] AFFF formulations have historically included some PFAAs (e.g., PFOS), but also a substantial portion of polyfluorinated substances that can be converted to PFAAs in the environment.[7,15] Because of their persistence, interactions with aquifer sediment via sorption will be fundamental in determining the fate

and transport of PFAAs in groundwater. Most previous studies have focused on equilibrium batch sorption of PFAAs to sediments, biosolids, and mineral surfaces, and under conditions specifically relevant to AFFF-impacted FPTAs.[16–19] Additionally, recent work investigated transport of PFOA in columns packed with sand under both saturated and unsaturated conditions, with the objective of understanding the impact of the air-water interface and co-contaminants on PFAS transport using a solid phase to which there is minimal sorption.[20,21] That data was re-examined along with data for PFOS to build a multi-process transport model, inclusive of rate-limited sorption.[22] Finally, column studies have examined how application of chemical oxidation remediation techniques and resulting alteration of subsurface conditions may influence transport of PFAAs;[23,24] however studies understanding the applicability of batch sorption studies to advective transport of PFAAs are limited.

Under water-saturated equilibrium conditions, PFAA transport is expected to decrease with increasing chain length for PFAAs with $CF_3(CF_2)_n$ –X, where $n \geq 4$.[16,19] Similar trends were observed in experiments that studied the leaching behavior of PFAAs from soil in flow-through column experiments.[25–27] However, sorption of some shorter PFAAs ($CF_3(CF_2)_n$ –X, where $n < 4$) in batch systems did not follow chain-length dependent trends with perfluorobutanoate (PFBA) exhibiting stronger sorption than perfluoropentanoate (PFPeA) or perfluorohexanoate (PFHxA).[19] Similarly, a field study that calculated sorption parameters (i.e. K_d) based on water and sediment concentrations found chain-length dependent trends in K_d only for $CF_3(CF_2)_n$ –X where $n \geq 6$.[28] Additional sorption trends include nonlinear (e.g. Freundlich) sorption and increasing sorption with increasing solid phase f_{oc}.[16,19]

In equilibrium transport, sorption is presumed to be instantaneous under the assumption that it occurs at much faster rates than the residence time of groundwater; however it has long been recognized that sorption of organic contaminants can be rate-limited, leading to nonequilibrium transport.[29–31] Various mechanisms have been proposed to explain rate-limited sorption behavior, typically involving interactions with organic matter such as organic matter diffusion.[32] Rate limited sorption behavior manifests itself in different ways depending on the scale of transport. In one-dimensional (1-D) flow through column experiments, when sorption is rate-limited, transport is sometimes characterized by early breakthrough and/or tailing of compound breakthrough curves (BTCs).[33] At larger scales, impacts are more uncertain but can lead to plume spreading, lower peak concentrations, and tailing.[33,34] Understanding rate limited sorption can have important implications for modeling plume behavior and evaluating remedial options.

Rate-limited sorption due to mass transfer limitations can be impacted by various compound properties. For many classes of neutral, nonpolar hydrophobic organic compounds (HOCs) the primary compound factors controlling mass transfer coefficients (k, see Section 2.6) are sorbate size and hydrophobicity, as evidenced by a single LFER that can describe an inverse relationship between log k and log K_d across various compound classes and sorbents ($\log k = 0.301 - 0.668 * logK_d, R^2 = 0.95$).[35] Deviations from the LFER occur for HOCs with complex functional groups or compounds with charged moieties. Pesticides (triazines) exhibit an approximately parallel LFER ($\log k = -0.55 - 0.57 * logK_d, R^2 = 0.89$) with lower k values (e.g. greater mass transfer limitations) despite their neutral charge,[36] and polar/anionic compounds also can be described with another approximately parallel (albeit less statistically robust) LFER ($\log k = -1.789 - 0.62 * logK_d, R^2 = 0.4$) with yet lower k values.[35] Decreasing k values in these compound classes are potentially caused by increased hindrance of

diffusion associated with more complex functional groups and/or specific interactions. HOC sorption is often considered to be dominated by van der Waals forces, but some neutral as well as anionic compounds may also exhibit specific interactions that increase mass transfer limitations relative to compounds that lack them.[35,36] Previous work also found that hydrocarbon alkyl tail length has an impact on mass transfer of HOCs in soils and polymers.[37,38] In these studies, k was inversely correlated with increasing tail length, up through propylbenzene in soil and pentane in a polymer. In soils, alkylbenzenes with increasing tail length followed the HOC LFER through 4-5 carbon chains, after which k remained constant. In both soils and polymers, tail length behavior was attributed to increasing hindrance to diffusion up through some critical tail length, beyond which the molecule becomes asymmetrical in shape. These results may also be relevant for $CF_3(CF_2)_n$ alkyl tails.

The effects of rate-limited sorption can be difficult to distinguish from other causes of nonequilibrium transport. Flow interruption column experiments, wherein flow through a column is stopped for a period of time (to allow conditions to progress towards sorbate-sorbent equilibrium) and then resumed, are useful in making a definitive determination of kinetic effects, including rate-limited sorption.[39–43] Flow interruption experiments are also often conducted at high pore-water velocities to experimentally exaggerate any kinetic effects. When compounds are recalcitrant or where compound transformation is prevented, drops in aqueous concentrations during the stop flow period can indicate physical or chemical nonequilibrium.[39] Nonreactive, conservative tracer tests are used to verify the absence of physical nonequilibrium in the column, such that drops in concentration of the compound of interest should confirm rate-limited sorption.

The objective of this work was to further the understanding of transport behavior of PFAAs in groundwater by investigating advective transport in 1-D saturated column experiments. Specifically, we conducted continuous flow column experiments at environmentally relevant pore-water velocities to determine if previously measured batch equilibrium data could be used to mathematically model 1-D PFAA transport. Flow interruption experiments were completed at higher pore water velocities to determine if rate-limited sorption influenced PFAA transport. Lastly, kinetic parameters were estimated with a combination of linear free energy relationships (LFERs) and mathematical modeling to evaluate factors that may lead to rate-limited PFAA sorption.

2. MATERIALS AND METHODS

2.1 Materials

Calibration standards (1-5,000 ng/L) of PFBA, PFPeA, PFHxA, perfluoroheptanoate (PFHpA), PFOA, perfluorononanoate (PFNA), perfluorodecanoate (PFDA), perfluorobutanesulfonate (PFBS), perfluorohexanesulfonate (PFHxS), and PFOS, as well as stable-isotope internal standards (Table S1) were purchased from Wellington Laboratories (Guelph, Ontario, Canada). Spiking solutions for all experiments were prepared from standards of PFAAs purchased from Sigma-Aldrich (St. Louis, MO). Stock solutions of calibration standards, spiking solutions (purity-corrected), and internal standards were prepared in a 70/30 (v/v) methanol/aqueous solution. All experiments utilized a spiking solution containing all 10 PFAAs. Potassium bromide was used as a nonreactive tracer. Unless otherwise specified, all other chemicals were of reagent grade and were purchased from Thermo Fisher Scientific (Waltham, MA), Mallinckrodt Pharmaceuticals (St. Louis, MO), or Sigma-Aldrich.

155

156 Solid phases used in this study were selected to represent a variety of geochemical and physical
157 characteristics (Table S2). Loamy Sand (A, f_{oc}=0.017) and Loam (B, f_{oc}= 0.045) were purchased from
158 Agvise Laboratories (Northwood, ND) and have been used by the authors in a previous batch
159 equilibrium sorption study.[19] Loamy Sand 2 (C) from an alluvial aquifer (Rifle, CO) was also used.
160 Lastly, this study included a silica sand (0.297 to 0.420 mm; Sand) (Accusands, Unimin Corp., Ottawa,
161 MN) which had been previously characterized.[44] Soils A and B were air dried and sieved (2mm) prior
162 to use in columns. Soil C and Sand were dry and able to pass through a 2mm sieve upon receipt.
163 Column aqueous phase for all experiments was artificial groundwater (AGW; deionized water with ions
164 typically found in groundwater; Table S3) utilized in previous studies.[19,23,24]
165

166 **2.2 Column Design**

167

168 All column experiments were conducted in 2.5 X 15 cm (No. 42400-2515) or 2.5 X 5 cm (No. 420400-
169 2505) Kontes ® glass chromatography columns (Kimble Chase, Vineland, NJ) with a fritted, glass bed
170 support in the influent end of the column. Shorter, 5 cm columns were selected for the continuous flow
171 column experiments to reduce the duration of these relatively longer experiments. Columns were
172 packed in 1-cm increments. Each increment was vibrated and tamped to establish uniform column
173 properties. Glass wool and 1-mm glass beads were used as additional bed support in caps at each end of
174 the column to fill void space, stabilize column packing material and establish uniform influent
175 distribution across the bed during column operation. Following packing, columns were saturated with
176 CO_2 to remove residual air and subsequently saturated with AGW in up-flow mode. Bulk density and
177 porosity of Soils A-C and Sand were determined gravimetrically (Table 1). Columns were attached to an

178 Ismatec ® high-accuracy peristaltic pump and silicone tubing (IDEX Health and Science, Oak Harbor,
179 WA). All columns were operated in up-flow mode and column influent/effluent samples were collected
180 from 3-way valves installed at each end of the column. PFAA losses (if present) that occurred to
181 column tubing were accounted for by sampling the inlet concentrations via the 3-way valve, which was
182 situated after the tubing. Further, specific surface areas of Soils A-C and Sand (~1-10^4 m^2)[45] in this
183 study are orders of magnitude higher than the glass surface area of the columns ($\leq 10^{-2}$ m^2) and tubing
184 (~10^{-3} m^2), and this work illustrates that sorption to silica sand (i.e. similar to glass beads) is minimal
185 (Table S9). Collectively this shows that losses of PFAAs to column materials will be minimal relative
186 to PFAA interaction with sorbents.
187
188 Prior to initiation of PFAA flow through experiments, nonreactive bromide (Br^-) tracer tests (Section S2
189 Tables S4 and S5) were completed to determine hydrodynamic transport conditions (Table 1) in all
190 columns and confirm the absence of physical nonequilibrium in flow interruption columns. Br^-
191 tracer tests were conducted at higher pore water velocities (2.7-11.8 m/day) than PFAAs, but this had
192 no adverse impact on the analysis because hydrodynamic properties were independent of flow rate under
193 all study conditions. In particular, based on a Peclet number analysis, diffusive transport was negligible,
194 and models of PFAA transport (discussed below) were insensitive to dispersivity, indicating that neither
195 process significantly influenced transport (e.g. advective processes dominated transport, see Section
196 S2). Following the completion of all column experiments, Br^- tests were repeated to ensure that column
197 properties remained consistent throughout the duration of the experiments (Figure S1).
198
199
200

Table 1 Summary of PFAA experimental conditions.

Column	Packing Type[1]	Column Length (cm)	Darcy Velocity (m/day)	Pore Water Velocity (m/day)	Bulk Density (g/cm^3)	Porosity	Experiment Type
1	Soil A	5	0.045	0.082	1.22	0.55	Continuous flow
2	Soil B	5	0.029	0.048	0.94	0.61	Continuous flow
3	Soil C	5	0.029	0.078	1.66	0.37	Continuous flow
4	Sand	5	0.045	0.115	1.77	0.39	Continuous flow
5	Soil A	15	0.412	0.698	1.04	0.59	Flow interruption
6	Soil C	15	0.412	1.177	1.65	0.35	Flow interruption
7	Sand	15	0.412	1.084	1.57	0.38	Flow interruption

[1]Packing material f_{oc}: Soil A = 0.017, Soil B = 0.045, Soil C = 0.0017, and Sand = 0.

2.3 PFAA Column Tests

Two types of saturated column experiments were used in this study to investigate PFAA transport (Section S3). Continuous flow column experiments (columns 1-4; Table 1) were used to study PFAA transport under environmentally relevant groundwater flow conditions. Flow interruption experiments (columns 5-7) were used to determine the impact of rate-limited sorption on PFAA transport. Higher flows were used for these experiments to maximize the possibility of observing a measurable result under the assumption that measured rate constants would apply generally, as observed in other flow interruption studies.[39] Column influent consisted of a PFAA mixture (~5 μg/L of each PFAA) prepared in AGW. During column experiments, influent concentrations varied only 2.9% (PFBS) – 13.3% (PFDA) from the mean. All column experiments were conducted using a mixture of 10 PFAAs, as previous work suggested that competitive effects of mixtures in soils used in this study are minimal,[19] and mixtures are more relevant to real-world PFAS releases.[7,8] Spiked AGW was injected in columns until the relative concentration (C/C_0) was ~1 for all PFAAs. In columns 5-7, flow was stopped when C/C_0 was ~ 1 for a period of 36 hrs. Following the flow interruption period, flow of spiked AGW was resumed until C/C_0 reached ~1 again. All columns were flushed with AGW until PFAA concentrations

returned to background following injection of spiked AGW (Table S5). Consistent with previous work, method of moments analysis was used to calculate mass recovery of all Br^- (Table S4) and PFAA BTCs (Table S6).[23,46]

2.4 Sample Preparation and Analysis

Column influent and effluent samples were collected manually in 2.0 mL polypropylene, microcentrifuge tubes and sample volumes were determined gravimetrically. An aliquot of isopropanol was added to comprise 9% of the aqueous volume in the tube. Samples were vortexed and centrifuged (AccuSpin Micro 17, Thermo Fisher Scientific) at 17,000 relative centrifugal force (RCF) for 30 minutes as a precaution to remove any residual suspended solids prior to direct injection. Next, 1,350 µL was transferred to an autosampler vial with 150 µL of 70/30 containing 0.3 ng internal standard (Table S1). Samples were analyzed directly via a MDS Sciex Applied Biosystems 3200 ™ (MDS Sciex, Ontario) liquid chromatography tandem mass spectrometer (LC-MS/MS), using methods modified from previous studies.[17,19,47] The LC-MS/MS was used to monitor two transitions for each analyte. Quantitation was performed using Analyst software (AB Sciex, Framingham, MA). Limits of quantitation were analyte and run-dependent but were approximately 2-9 ng/L. All values reported are corrected for recovery of internal standards (Section S1), which were generally greater than 60% for all samples and matrices.

2.5 Equilibrium PFAA Sorption

Equilibrium sorption coefficients for Soils A and B were measured in our previous work.[19] In some cases, the aqueous concentrations measured in column experiments was lower than the range evaluated

242 in sorption isotherms. To obtain isotherm parameters applicable to the entire range of concentrations in
243 this study, original isotherms were extended by linearly extrapolating the isotherm from the lowest
244 measured isotherm point to the lowest measured column concentration (Section S4, Figures S2-S4,
245 Table S7). PFAA sorption has been described by the Freundlich isotherm:[16,19]
246 $C_s = K_f C_w^n$, (1)
247 where C_s is the concentration in soil, C_w is the concentration in water, K_f is the Freundlich sorption
248 coefficient, and n is the linearity value. Values of n in previous work ranged from 0.7-1.1,[19] indicating
249 that nonlinearity is sometimes associated with PFAA sorption. In general, the lower portion of
250 Freundlich isotherms associated with higher energy sorption sites is linear,[48] so we consider linear
251 extrapolation of PFAA isotherm below the lowest measured point to be a reasonable assumption.
252
253 Studies measuring PFAA sorption to Soil C and Sand were not available, so limited 3-point sorption
254 isotherms (initial C_w of 0.5-50 µg/L) were completed using methods outlined in previous work (Section
255 S4).[19] PFAA isotherms were fit with the Freundlich isotherm to obtain K_f and n values (Table S9). As
256 in previous studies, PFAA mass recoveries in the solid and aqueous phases as well as loss to the vial
257 were used to complete mass balances in all batch reactors. In some cases, unacceptable mass balances
258 of PFAAs occurred due to over recovery in the lowest isotherm point (Table S9). When this occurred,
259 the low point was excluded from the isotherm. Resulting isotherm parameters should be considered
260 estimates. As with Soils A and B, the aqueous concentrations measured in the columns were in some
261 cases lower than the range of the isotherms, so linear extrapolation to the lowest measured column
262 concentration was applied (Section S4, Figures S2-S4, Table S7). The method for this extrapolation and
263 a detailed discussion of the extrapolation approaches considered is included in the Supplementary
264 Material (Section S4). Neither extrapolation of parameters nor elimination of the lowest isotherm point

265 led to substantial changes in isotherm parameters applied in Soil C or Sand, as sorption of the majority
266 of PFAAs to these solid phases was approximately linear.
267
268 **2.6 Data Analysis**
269
270 BTCs (C/C_0 vs. time) for Br^- were modeled using the nonlinear, least-squares model CFITM.[49] BTCs
271 for PFAAs were fit with a numerical solution to the advection-dispersion equation (ADE) using
272 HYDRUS-1D.[50] Dispersivities (Table S4) were determined from inverse fits of Br^- tracer tests and
273 utilized when modeling breakthrough of PFAAs in HYDRUS 1-D. HYDRUS 1-D was used in both
274 inverse and forward modeling of PFAA transport because it was capable of simulating flow interruption
275 experiments. Equilibrium sorption parameters K_f and n from batch experiments were used to predict
276 PFAA breakthrough in columns, and results were compared to measured BTCs. All sorption
277 parameters were from batch experiments using the same PFAA mixture employed in column studies,
278 which would account for any minor competitive effects of single vs. mixed solute systems. Where
279 applicable, BTCs were subsequently fit with a two-site model that assumes sorption sites can be divided
280 into two fractions and incorporated into the ADE.[51] In this model, C_s is assumed to be a combination of
281 solid phase concentrations on Type 1 sites (C_s^e, mg/kg) and Type 2 sites (C_s^k, mg/kg). For Type 1 and
282 Type 2 sites respectively:
283 $$C_s^e = fC_s = fK_f C_w^n \qquad (2)$$
284 $$C_s^k = (1-f)C_s = (1-f)K_f C_w^n \qquad (3)$$
285 where f is the fraction of sorption sites assumed to be at equilibrium with the solute. The sorption rate
286 for Type 1 sites is assumed to be instantaneous and can be described as follows:
287 $$\frac{\partial C_s^e}{\partial t} = f\frac{C_s}{\partial t}. \qquad (4)$$

Sorption onto Type 2 sites is assumed to be a first order rate process:

$$\frac{\partial C_s^k}{\partial t} = k\left[(1-f)K_f C_w^n - C_{s,t}^k\right], \qquad (5)$$

where $C^k_{s,t}$ is Type 2 solid phase concentration at time t and k is the mass transfer coefficient (min^{-1}). Modeling efforts focused on Br^- and PFAA results from continuous flow experiments as well as Br^- results from flow interruption data. Linear free energy relationships (LFERs) from previous work[35] and K_d values this and previous work[19] were used to estimate k values. As will be discussed, PFAA flow interruption BTCs were insufficient for use in obtaining modeled (i.e. fitted) parameters, so they were used solely for verification of rate-limited sorption effects and kinetic parameters were determined from LFERs.

3. RESULTS AND DISCUSSION

3.1 Trends with Chain Length and f_{oc}

Sorption parameters from batch equilibrium studies were used to model expected PFAA BTCs in columns. Modeled BTCs yielded information on the expected order of PFAA breakthrough based on compound chain length and soil f_{oc}, which are two primary factors found to influence sorption in batch studies,[16,19] although studies suggest that trends with f_{oc} are not consistent across all soil types.[52] The modeled order of breakthrough was then compared to the order of breakthrough observed in column data (Figures S5-S8). This initial analysis focuses on trends (i.e. order of breakthrough) associated with chain length and f_{oc} in modeled vs. measured data. The analysis is supported by data shown in Figures S5-S9, which are scaled to show only very early breakthrough times to enable observation of the trends

310 discussed herein. A direct comparison of full BTCs with equilibrium models is presented in Figures S5-
311 S8 (panel G), Section 3.2, Figure 1, and Figures S10-S13.
312
313 *3.1.1 Trends with Chain Length.* Equilibrium (model predicted) BTCs exhibited chain length dependent
314 trends only in Soils A-C (f_{oc} = 0.0017-0.045, Figures S5-S7 A, C, and E). Some exceptions to chain
315 length trends were observed in Soils C and Sand, but these may be an artifact of using estimated isotherm
316 parameters for these sorbents (Figure S8 A, C, and E). Batch sorption observations of stronger PFBA
317 sorption relative to PFPeA and PFHxA[19] were not evident when applied to modeled predictions of 1-D
318 advective transport. In measured data, chain-length dependent trends for compounds with $CF_3(CF_2)n$ –X
319 where $n \geq 4$ were most evident in Soil B experimental BTCs (highest f_{oc}, Figure S6 B, D, and E).
320 Compound elution appeared nearly simultaneous in the remaining solid phases for perfluoroalkyl
321 carboxylates smaller than PFDA and perfluoroalkyl sulfonates smaller than PFOS (e.g. Figure S5, S6,
322 and S7 B, F). In many cases, breakthrough appeared to be a close approximation of conservative (non-
323 sorbing) transport (e.g. Figure S7 B). As in models, anomalous trends in PFBA and PFPeA sorption
324 were not evident in measured column data. This may be attributable to the nonlinear sorption of PFBA
325 relative to PFPeA (n=0.65-0.8 for PFBA vs. 0.84-1.01 for PFPeA). A compound with a high K_f value
326 and n<1 may exhibit slower transport (i.e. greater retardation) at low concentrations relative to a
327 compound with a low K_f and $n \approx 1$.
328
329 *3.1.2 Trends with f_{oc}.* Organic carbon-dependent sorption was evident in models to a degree:
330 breakthrough of a given PFAA in Soils A, C, and Sand (f_{oc} = 0-0.017) was predicted to occur at similar
331 times, but breakthrough was later in Soil B, which had the highest f_{oc} (f_{oc} = 0.045). For example, PFNA
332 breakthrough was predicted to occur at 0.5 pore volumes in Soil A (Figure S5C), 2.4 pore volumes in

Soil C (Figure S7C), 1.4 pore volumes in Sand (Figure S8C), and 5.2 pore volumes in Soil B (Figure S6C). In measured data, BTCs of PFNA, PFDA, and PFOS exhibited f_{oc}-dependent breakthrough (Figure S9), but smaller compounds did not show a trend with f_{oc}. Deviations of column behavior from modeled transport are further discussed in Section 3.2

3.2 Evaluation of Equilibrium Transport

Predicted equilibrium and measured BTCs were compared (Table 2, Figure 1, Figures S10-S13), visually inspected for signs of nonequilibrium transport (e.g. early breakthrough and/or tailing), and statistically evaluated using coefficients of determination (R^2, Table S8-S9) and residuals between predicted and observed values (Figure S14). Two factors were applied to screen BTCs and identify those that should be further evaluated for nonequilibrium breakthrough: visual inspection and BTCs with $R^2<0.7$. The latter was included to identify BTCs that should be targeted for further investigation due to relatively poorer fits (low R^2) despite a lack of visual evidence (early breakthrough, tailing) of nonequilibrium transport. Table 2 summarizes these *screening* results (see columns labeled 'Screening Observation'). Screening observations are not a final determination of equilibrium or nonequilibrium transport for each PFAA-sorbent combination. Our conclusion regarding each BTC is also summarized in Table 2 (see columns labeled 'Conclusion) as discussed further below. Collectively, screening results yield four types of BTCs: early breakthrough (Type I), early breakthrough and tailing (Type II), late breakthrough and tailing (Type III), and no observable early breakthrough or tailing (Type IV). Nonequilibrium transport may be caused by several factors including nonlinear and rate-limited sorption.[30] Nonlinear sorption was addressed by use of Freundlich sorption parameters when modeling predicted breakthrough. Type II behavior is consistent with rate-limited sorption,[30] and is further

356 discussed in Section 3.3. Potential causes of Types I, III, and IV behavior are discussed in more detail

357 below.

358

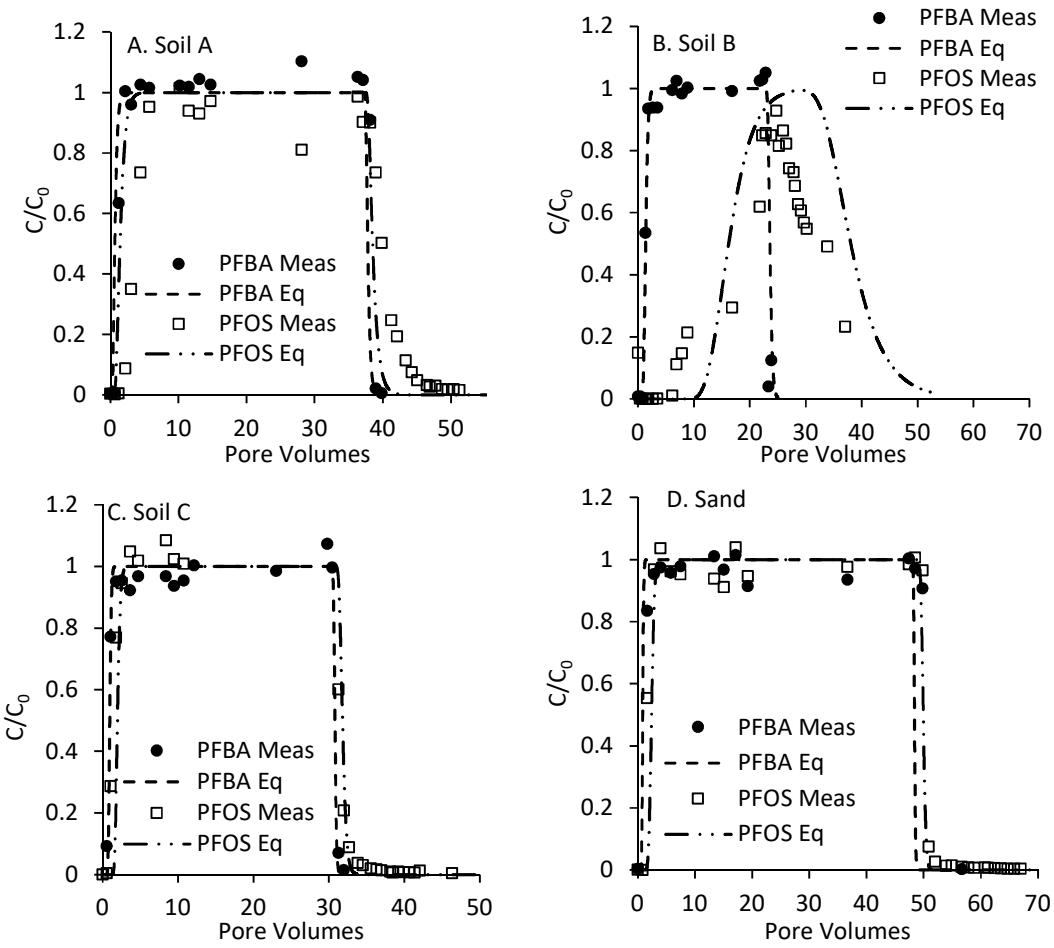

Figure 1. Predicted equilibrium (Eq) transport and measured (Meas) breakthrough of PFBA and PFOS in a.) Soil A (R^2 PFBA=0.7, R^2 PFOS=0.64) b.) Soil B (R^2 PFBA=0.38, R^2 PFOS=0.29), c.) Soil C (R^2 PFBA=0.98, R^2 PFOS=0.9), and d.) Sand (R^2 PFBA=0.15, R^2 PFOS=0.9).

Table 2. Results of initial screening to identify PFAA BTCs meriting further evaluation and conclusions once additional evaluation was complete.

	Soil A (f_{oc} = 0.017)			Soil B (f_{oc}=0.045)			Soil C (f_{oc} = 0.0017)			Sand (f_{oc} = 0)		
PFAA	**Screening Observation**	**R^2**	**Conclusion**	**Screening Observation**	**R^2**	**Conclusion**	**Screening Observation**	**R^2**	**Conclusion**	**Screening Observation**	**R^2**	**Conclusion**
PFBA	Equilibrium	0.70	Equilibrium	Equilibrium	0.40	Equilibrium	Equilibrium	0.96	Equilibrium	Equilibrium	-0.06	Equlibrium
PFPeA	Equilibrium	0.70	Equilibrium	Early	-0.25	Equilibrium	Early	-0.08	Equilibrium	Equilibrium	0.59	Equlibrium
PFHxA	Equilibrium	0.88	Equilibrium	Equilibrium	0.78	Equilibrium	Early	0.73	Equilibrium	Equilibrium	0.59	Equlibrium
PFHpA	Equilibrium	0.96	Equilibrium	Early, tailing	0.53	N/A	Early	0.56	Equilibrium	Equilibrium	0.52	Equlibrium
PFOA	Equilibrium	0.95	Equilibrium	Early, tailing	0.05	N/A	Early	0.48	Equilibrium	Equilibrium	0.85	Equlibrium
PFNA	Equilibrium	0.90	Equilibrium	Early, tailing	-0.86	N/A	Early, tailing	0.10	Rate-limited	Equilibrium	0.84	High flow RL
PFDA	Late, tailing	0.31	Rate-limited, other	Late, tailing	-4.01	N/A	Early, tailing	0.53	Rate-limited	Equilibrium	0.93	Equlibrium
PFBS	Equilibrium	0.91	Equilibrium	Early	0.65	Equilibrium	Early	0.75	Equilibrium	Equilibrium	0.39	Equlibrium
PFHxS	Equilibrium	0.94	Equilibrium	Equilibrium	0.81	Equilibrium	Early	0.80	Equilibrium	Equilibrium	0.39	Equlibrium
PFOS	Late, tailing	0.69	Rate-limited, other	Early, tailing	0.26	N/A	Early	0.88	High flow RL	Equilibrium	0.91	High flow RL

Notes: Screening observations result from initial screening of BTCs as described in Section 3.2 Conclusions were made following additional consideration of uncertainty in sorption parameters (Section 3.2.1) and flow interruption data (Section 3.3). N/A indicates that conclusions are not provided for some compounds in soil B due to the failure of flow interruption experiments. Late denotes breakthrough later than equilibrium predictions; Early denotes breakthrough earlier than equilibrium predictions; Equilibrium denotes no evidence of early/late breakthrough or tailing. Types of BTCs: Type I (yellow) exhibited early breakthrough, Type II (gray) exhibited early breakthrough and tailing, Type III (blue) exhibited late breakthrough and tailing, and Type IV (green) exhibited no observable early/late breakthrough or tailing but $R^2 < 0.7$. All unshaded values exhibited no visual or statistical evidence of nonequilibrium behavior.

3.2.1 Types I and IV BTCs. Types I and IV breakthrough were collectively characterized by low R^2 values, slight to no early breakthrough, and no tailing (Table 2). Applicability of either an equilibrium or a rate-limited sorption assumption to these BTCs was initially unclear. Inspection of residuals (squared difference between predicted and measured values at each measured point, examples provided in Figure S14) illustrates that low R^2 values in the majority of these cases were caused by a single measured point in the arrival wave that reached a relative concentration of unity earlier than expected and/or a single measured point that eluted slightly faster (was lower) than expected, indicating a slight shift that might be caused by lower-than-expected sorption (e.g. Figure S14). If these individual points are removed from the statistical analysis, R^2 values for these cases are greater than 0.9. Small deviations in equilibrium sorption parameters may have contributed to these trends. This point is illustrated by considering sorption of PFHpA in Soil C. When the variability (i.e. standard deviation) of measured soil and aqueous phase concentrations in the isotherms was considered, Log K_f (approximately equivalent to linear sorption in this case, as n=0.99) range from -0.62 to -0.37. Initially, a log K_f value of -0.48 was used to predict equilibrium PFHpA sorption to Soil C resulting in an R^2 value of 0.56 when compared to measured data (Table 2). When predictions were repeated with the minimum potential Log K_f of -0.62, the resulting comparison to measured data resulted in an R^2 of 0.71. Additionally, isotherm parameters for Soil C and Sand were considered estimates. Collectively, this suggests that Types I and IV BTCs may be due to the variability of the equilibrium isotherm parameters (and potentially analytical variability) and/or an artifact of the estimated isotherm parameters, as opposed to nonequilibrium transport (Table 2).

3.2.2 Type III BTCs. For Type III behavior, the cause of late breakthrough of PFDA and PFOS is unclear, but the data suggest that sorption of these compounds was stronger than measured in

393 equilibrium systems. The fact that this occurred for only these two compounds and only in Soils A and
394 B (f_{oc} = 0.017 and 0.045, respectively) suggests a relationship with chain length and f_{oc}. Unlike Types I
395 and IV, variability in K_f and n values measured in batch systems[19] could not entirely account for the
396 increased sorption observed in columns. Recent studies of PFAS sorption to anion exchange resins used
397 transmission electron microscopy (TEM) images to illustrate that resins saturated with PFOA at a
398 concentration of 1 mg/L developed 30-200 nm aggregates.[53] The authors hypothesized aggregates
399 represented PFOA hemimicelles formed at the resin surface. A separate study also noted the potential
400 for micelle or agglomeration to impact sorption of long-chain PFAAs to granular activated carbon.[54]
401 The critical micelle concentration (CMC) of PFOA is approximately 3,540 mg/L[55] and hemimicelle
402 formation is possible at 0.001-0.01 of the CMC[48] or a minimum of 3.5 mg/L which is in the same order
403 of magnitude as concentrations where aggregates were observed.[53] The CMCs for PFDA and PFOS in
404 water are approximately 400 and 3,151 mg/L at 25°C,[55,56] respectively, though values are dependent on
405 factors such as counterions and solution chemistry.[1] Hemimicelle formation would be possible at
406 minimum concentrations of 0.4 mg/L for PFDA and 3 mg/L for PFOS, which is 80-600 times higher
407 than influent PFAA concentrations in this study. However, column experiments were conducted using
408 PFAA mixtures (10 PFAAs at ~5 μg/L each) including PFUnA, which has the lowest CMC of those
409 included in the study. Impacts of mixtures on PFAA hemimicelle formation are currently unknown.
410 Since hemimicelle formation would likely be driven by the lower CMCs and stronger hydrophobic
411 interactions of PFDA and PFOS relative to smaller PFAAs, this would explain why late breakthrough
412 was only observed in PFOS and PFDA in soils with higher f_{oc}. Additional experiments would be needed
413 to determine the underlying cause of Type III BTCs.
414
415

3.3 Flow Interruption Experiments

Preliminary evaluation of equilibrium transport in continuous flow experiments showed potential for nonequilibrium PFAA transport. Flow interruption experiments were completed with Soils A, C, and Sand to further investigate if rate-limited sorption led to these observations. Soil B flow interruption experiments were attempted, but the fine-grained nature of the soil led to overpressure and failure of the columns. Prior to initiation of PFAA tests, flow interruption experiments were completed with Br^- to ensure physical nonequilibrium (resulting from diffusive mass transfer between mobile and immobile regions) was not evident within the columns.[39] Nonequilibrium was not observed in any of the flow interruption Br^- tests (Figure S15); therefore, any concentration drops observed in subsequent PFAA flow interruption experiments were solely attributed to rate-limited sorption.

For a perturbation during the flow interruption period to be considered a concentration decrease, the measured concentration following the stop-flow period had to be lower than the lowest concentration measured after the columns reached a relative concentration (C/C_0) of 1. Decreases in PFAA concentrations during the stop flow period (36 hrs) for high flow (Table 1) scenarios were observed for: PFDA and PFOS in Soil A; PFNA, PFDA, PFHxS, and PFOS in Soil C; and PFDA and PFOS in Sand (Figure 2, Figures S16-S18). This illustrates that rate-limited sorption impacts transport of these compounds during flow interruption experiments (Table 2). It also suggests that continuous flow, Type II BTCs for PFNA and PFDA in Soil C and Type III BTCs for PFDA and PFOS in Soil A were at least partially caused by rate-limited sorption, though, as discussed, rate-limited sorption does not typically result in late breakthrough (i.e., Type III behavior, see Table 2). Despite flow interruption experiments exhibiting rate-limited sorption for PFDA in Sand, and PFHxS and PFOS in Soil C and Sand, these were

well described by equilibrium transport in the corresponding continuous flow experiments. Previous studies have observed rate-limited sorption of organic contaminants in low organic carbon sorbents as well as PFOA and PFOS in sand.[22,57] It is possible that at the low flow rates used in the continuous flow experiments, equilibrium conditions apply, but kinetic impacts occurred at the higher flow rates used in the flow interruption experiments. A lack of perturbation in concentrations during stop flow periods for PFAAs exhibiting Type I and II behavior in continuous flow BTCs further illustrates that those compounds primarily undergo equilibrium transport (Table 2).

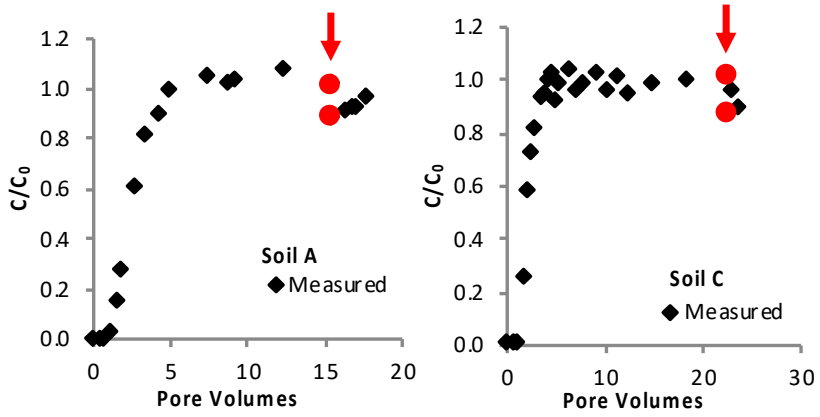

Figure 2. Flow interruption data PFOS in Soil A and Soil C. Data points collected immediately prior to and following the stop flow period are shown in red to facilitate observation of any observed drops in concentration.

While flow interruption experiments confirmed rate-limited sorption of some PFAAs, quantitative analysis of kinetic parameters associated with this process is useful for fate and transport predictions. Ideally, changes in C_w during the stop flow period can be modeled using inverse methods to parameterize f and k values associated with the process.[39] However, in this data set, the degree of scatter in the data around $C/C_0=1$ made it difficult to quantify with certainty the magnitude of the drop in

453 concentration during flow interruption. As a result, kinetic parameters were not obtained from that data.
454 Nevertheless, flow experiments do confirm rate-limited impacts on PFAA transport.
455
456 **3.4 Factors Impacting PFAA Mass Transfer**
457
458 Herein, we used a 2-site sorption model to understand nonequilibrium transport of PFAAs due to rate-
459 limited sorption (Equations 2-5), where equilibrium sorption parameters are used in conjunction with a
460 mass transfer coefficient (k) and a fraction of type 1 sorption sites (f) to describe compound
461 breakthrough. The model does not carry implicit assumptions in the fundamental processes resulting in
462 mass transfer limitations, which could arise from multiple mechanisms.[32,35,58] Determination of the
463 specific diffusive mechanism or combination of mechanisms only becomes important when trying to
464 quantitatively translate k values or explain certain qualitative trends.[38] Determination of specific
465 diffusive mechanisms leading to PFAA transport was not an objective of this study. If a combination of
466 mechanisms contributes to rate-limited PFAA transport, k values in the 2-site sorption model would
467 represent overall mass transfer limitations caused by these effects.
468
469 As noted, kinetic parameters could not be obtained from flow interruption data, and an attempt was also
470 made to use optimization techniques to obtain kinetic parameters from continuous flow experiments and
471 compare them to LFERs. Resulting model fits were not unique, which may be due to scatter in BTCs
472 and/or low overall sorption (e.g. $R \approx 1$). To further investigate the significance of rate-limited PFAA
473 transport, values of k were estimated using the LFER for polar/anionic compounds (Table S10).[35] This
474 was done using K_d values for PFHpA, PFOA, and PFNA in Soil B because they exhibited Type II BTCs
475 and PFNA and PFDA in Soil C, because rate-limited sorption was confirmed in flow interruption

476 experiments. Sorption of these compounds in Soils B and C was approximately linear (n=0.95-1.03), so
477 $K_f \approx K_d$. This method of estimating k could not be applied to other rate-limited compounds (PFDA and
478 PFOS in Soils A and B) because these compounds exhibited enhanced sorption relative to what was
479 expected in batch systems, rendering equilibrium sorption parameters invalid for describing
480 breakthrough. After k values were estimated from the LFER, they were applied to continuous flow
481 experiments and values of f were determined through model optimization (Table S9). In all cases, the
482 resulting kinetic parameters improved predictions of breakthrough relative to models assuming
483 equilibrium sorption (Figure 3, Figure S19). To test the robustness of the resulting kinetic parameters
484 and their independence from pore water velocity, resulting values of k and f were applied to predict
485 observed flow interruption BTCs prior to the stop flow period. Since Soil B flow interruption
486 experiments failed, this was only possible for kinetic parameters for PFNA and PFDA in Soil C.
487 Results show that estimated parameters were capable of predicting PFAA breakthrough at higher pore
488 water velocities (Figure S19).
489
490 Values of k were estimated using the LFER for polar/anionic compounds[35] because neither the HOC nor
491 pesticide LFERs[36] were capable of predicting k values that fully captured observed breakthrough.
492 Implicit in this LFER is some combination of either increased diffusive hindrance or specific
493 interactions relative to the 'base' LFER for HOCs. Although PFAAs were not included in the set of
494 compounds used to develop this LFER, diffusive hindrance due to anionic moieties may extend to
495 PFAAs. This is in contrast to LFERs for other properties such as pKa, where unique PFAA properties
496 (e.g. inductive effects) can only be captured by use of relevant compounds in LFER development.
497 Previous research has suggested that specific interactions do not play a significant role in PFAA sorption
498 and that the process is the result of a combination of hydrophobic and electrostatic interactions.[59] Since

499 electrostatic interactions (e.g. interactions with metal oxides in clay) are not likely to be rate limiting,
500 this may mean increased hindrance causes slower PFAA mass transfer relative to HOCs. However,
501 more work is needed to understand this fully. This work also did not explore potential for k values to
502 become constant above some critical fluorocarbon alkyl tail length. As mentioned (see Introduction),
503 previous work implies that there may be a critical hydrocarbon chain length beyond which k values will
504 not decrease further,[37,38] but it is unknown if this critical point would be the same for perfluoroalkyl
505 tails. Additionally, this effect is likely to be most relevant to polymer models (i.e. intrasorbent
506 diffusion), and the exact rate-limited mechanisms that apply to PFAAs have not been determined.
507
508 Fitted values of f (i.e. fraction of Type 1 sorption sites) in this study were found to increase with
509 increasing chain length (Table S9). This is consistent with previous work that found values of f for a
510 series of HOCs were shown to increase with increasing K_{ow}, used as a proxy for molecular size.[60,61]
511 This is possibly due to an inability of larger compounds to access some of the internal organic matter
512 sites typically attributed to rate-limited behavior. Therefore, of all sorption sites available to these
513 compounds, larger fractions are represented by external, instantaneous sorption sites relative to a
514 compound of smaller size.[60] It should be emphasized that values of f and k determined in this study are
515 estimates and were developed to help draw inferences about the significance of rate-limited behavior to
516 overall PFAA transport. Additional work would be required to confirm their broader applicability.

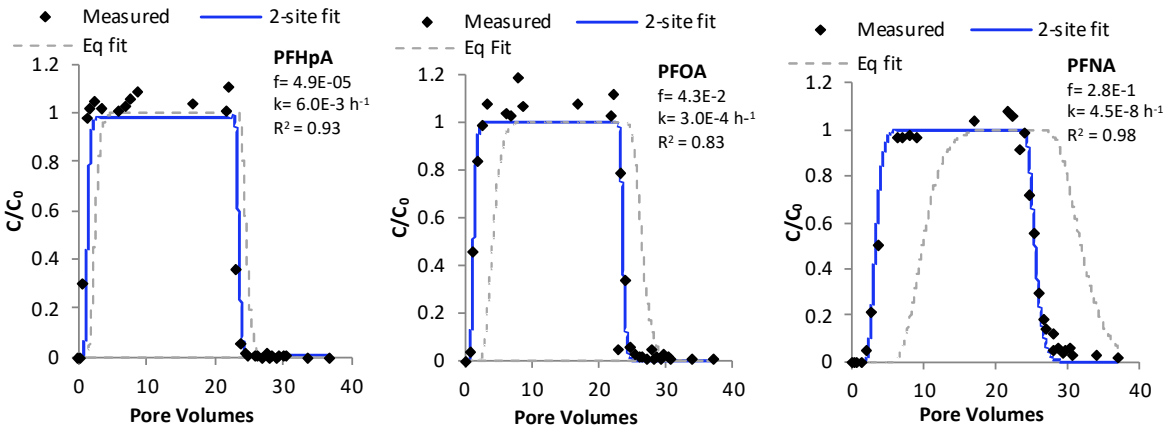

Figure 3. Measured continuous flow data and modeled breakthrough using calculated k values and optimized values of f (2-site fit) for PFHpA, PFOA, and PFNA in Soil B compared to the equilibrium sorption mode (Eq fit). Resulting R^2 values show improved correlation of the 2-site fit compared to the Eq fit (R^2 0.21-0.59). PFHpA breakthrough appears to occur slightly early, but when the standard deviation of sorption parameters is considered, breakthrough is within the resulting window of equilibrium transport, similar to trends described for Type I BTCs.

4. CONCLUSIONS

This study illustrates that breakthrough of some PFAAs is not well represented by applying equilibrium sorption parameters and that rate-limited sorption considerations are needed to fully capture 1-D transport of some PFAA/sorbent combinations at environmentally relevant pore water velocities. However, relevance of this behavior at field scales needs to be validated. Transport at the field scale will be 3-D and subsurface conditions are likely to be heterogeneous relative to column transport. These factors may be more important in determining overall field transport of PFAAs as with other HOCs.[60] Nonetheless, rate-limited processes have been shown to be helpful at both explaining field-scale behavior and simulating field-scale data, even in physically heterogeneous conditions.[33] Before reaching the saturated zone, PFAA transport will be influenced by the air-water interface in the vadose

zone.[20,62] Additionally, AFFF-impacted areas are likely to have other complicating factors. At FPTAs, AFFF impacts are likely due to multiple releases during repeat training exercises. Further, AFFF formulations vary, and multiple foam types may have been used. Some AFFF formulations include PFASs other than PFAAs, some of which can serve as PFAA precursors that transform into PFAAs over time.[63,64] Thus, nonideal PFAA transport at field scales may include effects of rate-limited sorption, complex subsurface characteristics, enhanced retardation in the vadose zone, multiple releases, and PFAA precursor transformation.[22] Additional work is needed to understand which of these factors are significant in modeling PFAA transport at the field-scale. As models are further developed, kinetic parameters determined in this work may serve as a tool for estimating relative contributions of rate-limited sorption to PFAA transport and overall need for (or lack thereof) more accurate measurements of kinetic parameters and an increased understanding of underlying mechanisms causing PFAA mass transfer limitations.

ACKNOWLEDGEMENTS

We acknowledge funding for this research from the Strategic Environmental Research and Development Program (SERDP ER2126). We would also like to acknowledge David Azzolini, Erica McKenzie, Evan Gray, KC Hyland, and Bridget Ulrich for their help in designing column experiments and collecting column samples.

REFERENCES

(1) Kissa, E. *Fluorinated Surfactants and Repellents, Second Edition Revised and Expanded*; Hubbard, A. T., Ed.; Surfactant Science Series; Marcel Dekker, Inc.: New York, NY, 2001.
(2) Anderson, R. H.; Long, G. C.; Porter, R. C.; Anderson, J. K. Occurrence of Select Perfluoroalkyl Substances at U.S. Air Force Aqueous Film-Forming Foam Release Sites Other than Fire-

Training Areas: Field-Validation of Critical Fate and Transport Properties. *Chemosphere* **2016**, *150*, 678–685. https://doi.org/10.1016/j.chemosphere.2016.01.014.
(3) USEPA. *Drinking Water Health Advisory for Perfluorooctane Sulfonate (PFOS)*; EPA 822-R-16-004; Office of Water Health and Ecological Criteria Division: Washington, DC, 2016.
(4) USEPA. *Drinking Water Health Advisory for Perfluorooctanoic Acid (PFOA)*; EPA 822-R-16-005; Office of Water Health and Ecological Criteria Division: Washington, DC, 2016.
(5) Moody, C. A.; Hebert, G. N.; Strauss, S. H.; Field, J. A. Occurrence and Persistence of Perfluorooctanesulfonate and Other Perfluorinated Surfactants in Groundwater at a Fire-Training Area at Wurtsmith Air Force Base, Michigan, USA. *J Env. Monit* **2003**, *5* (2), 341–345. https://doi.org/10.1039/b212497a.
(6) Schultz, M. M.; Barofsky, D. F.; Field, J. A. Quantitative Determination of Fluorotelomer Sulfonates in Groundwater by LC MS/MS. *Env. Sci Technol* **2004**, *38* (6), 1828–1835. https://doi.org/10.1021/es035031j.
(7) McGuire, M. E.; Schaefer, C.; Richards, T.; Backe, W. J.; Field, J. A.; Houtz, E.; Sedlak, D. L.; Guelfo, J. L.; Wunsch, A.; Higgins, C. P. Evidence of Remediation-Induced Alteration of Subsurface Poly- and Perfluoroalkyl Substance Distribution at a Former Firefighter Training Area. *Environ. Sci. Technol.* **2014**, *48* (12), 6644–6652. https://doi.org/10.1021/es5006187.
(8) Weber, A. K.; Barber, L. B.; LeBlanc, D. R.; Sunderland, E. M.; Vecitis, C. D. Geochemical and Hydrologic Factors Controlling Subsurface Transport of Poly- and Perfluoroalkyl Substances, Cape Cod, Massachusetts. *Environ. Sci. Technol.* **2017**, *51* (8), 4269–4279. https://doi.org/10.1021/acs.est.6b05573.
(9) Shin, H.-M.; Vieira, V. M.; Ryan, P. B.; Detwiler, R.; Sanders, B.; Steenland, K.; Bartell, S. M. Environmental Fate and Transport Modeling for Perfluorooctanoic Acid Emitted from the Washington Works Facility in West Virginia. *Environ. Sci. Technol.* **2011**, *45* (4), 1435–1442. https://doi.org/10.1021/es102769t.
(10) Moody, C. A.; Field, J. A. Determination of Perfluorocarboxylates in Groundwater Impacted by Fire-Fighting Activity. *Env. Sci Technol* **1999**, *33* (16), 2800–2806. https://doi.org/10.1021/es981355+.
(11) Place, B. J.; Field, J. A. Identification of Novel Fluorochemicals in Aqueous Film-Forming Foams Used by the US Military. *Environ. Sci. Technol.* **2012**, *46* (13), 7120–7127. https://doi.org/10.1021/es301465n.
(12) Giesy, J. P.; Kannan, K. Peer Reviewed: Perfluorochemical Surfactants in the Environment. *Environ. Sci. Technol.* **2002**, *36* (7), 146A-152A. https://doi.org/10.1021/es022253t.
(13) Giesy, J. P.; Kannan, K. Global Distribution of Perfluorooctane Sulfonate in Wildlife. *Environ. Sci. Technol.* **2001**, *35* (7), 1339–1342. https://doi.org/10.1021/es001834k.
(14) Park, S.; Lee, L. S.; Medina, V. F.; Zull, A.; Waisner, S. Heat-Activated Persulfate Oxidation of PFOA, 6:2 Fluorotelomer Sulfonate, and PFOS under Conditions Suitable for in-Situ Groundwater Remediation. *Chemosphere* **2016**, *145*, 376–383. https://doi.org/10.1016/j.chemosphere.2015.11.097.
(15) Houtz, E. F.; Higgins, C. P.; Field, J. A.; Sedlak, D. L. Persistence of Perfluoroalkyl Acid Precursors in AFFF-Impacted Groundwater and Soil. *Environ. Sci. Technol.* **2013**, *47* (15), 8187–8195. https://doi.org/10.1021/es4018877.
(16) Higgins, C. P.; Luthy, R. G. Sorption of Perfluorinated Surfactants on Sediments. *Env. Sci Technol* **2006**, *40* (23), 7251–7256. https://doi.org/10.1021/es061000n.

(17) Sepulvado, J.; Blaine, A.; Hundal, L. S.; Higgins, C. P. Occurrence and Fate of Perfluorochemicals in Soil Following the Land Application of Municipal Biosolids. *Env. Sci Technol* **2011**, *45* (19), 8106–8112. https://doi.org/10.1021/es103903d.
(18) Tang, C. Y.; Fu, Q. S.; Gao, D. W.; Criddle, C. S.; Leckie, J. O. Effect of Solution Chemistry on the Adsorption of Perfluorooctane Sulfonate onto Mineral Surfaces. *Water Res* **2010**, *44* (8), 2654–2662. https://doi.org/10.1016/j.watres.2010.01.038.
(19) Guelfo, J. L.; Higgins, C. P. Subsurface Transport Potential of Perfluoroalkyl Acids at Aqueous Film-Forming Foam (AFFF)-Impacted Sites. *Environ. Sci. Technol.* **2013**, *47* (9), 4164–4171. https://doi.org/10.1021/es3048043.
(20) Lyu, Y.; Brusseau, M. L.; Chen, W.; Yan, N.; Fu, X.; Lin, X. Adsorption of PFOA at the Air–Water Interface during Transport in Unsaturated Porous Media. *Environ. Sci. Technol.* **2018**, *52* (14), 7745–7753. https://doi.org/10.1021/acs.est.8b02348.
(21) Brusseau, M. L.; Yan, N.; Van Glubt, S.; Wang, Y.; Chen, W.; Lyu, Y.; Dungan, B.; Carroll, K. C.; Holguin, F. O. Comprehensive Retention Model for PFAS Transport in Subsurface Systems. *Water Res.* **2019**, *148*, 41–50. https://doi.org/10.1016/j.watres.2018.10.035.
(22) Brusseau, M. L. Simulating PFAS Transport Influenced by Rate-Limited Multi-Process Retention. *Water Res.* **2020**, *168*, 115179. https://doi.org/10.1016/j.watres.2019.115179.
(23) McKenzie, E. R.; Siegrist, R. L.; McCray, J. E.; Higgins, C. P. Effects of Chemical Oxidants on Perfluoroalkyl Acid Transport in One-Dimensional Porous Media Columns. *Environ. Sci. Technol.* **2015**, *49* (3), 1681–1689. https://doi.org/10.1021/es503676p.
(24) McKenzie, E. R.; Siegrist, R. L.; McCray, J. E.; Higgins, C. P. The Influence of a Non-Aqueous Phase Liquid (NAPL) and Chemical Oxidant Application on Perfluoroalkyl Acid (PFAA) Fate and Transport. *Water Res.* **2016**, *92*, 199–207. https://doi.org/10.1016/j.watres.2016.01.025.
(25) Gellrich, V.; Stahl, T.; Knepper, T. P. Behavior of Perfluorinated Compounds in Soils during Leaching Experiments. *Chemosphere* **2012**, *87* (9), 1052–1056. https://doi.org/10.1016/j.chemosphere.2012.02.011.
(26) Stahl, T.; Riebe, R. A.; Falk, S.; Failing, K.; Brunn, H. Long-Term Lysimeter Experiment To Investigate the Leaching of Perfluoroalkyl Substances (PFASs) and the Carry-over from Soil to Plants: Results of a Pilot Study. *J. Agric. Food Chem.* **2013**, *61* (8), 1784–1793. https://doi.org/10.1021/jf305003h.
(27) Vierke, L.; Möller, A.; Klitzke, S. Transport of Perfluoroalkyl Acids in a Water-Saturated Sediment Column Investigated under near-Natural Conditions. *Environ. Pollut.* **2014**, *186*, 7–13. https://doi.org/10.1016/j.envpol.2013.11.011.
(28) Labadie, P.; Chevreuil, M. Partitioning Behaviour of Perfluorinated Alkyl Contaminants between Water, Sediment and Fish in the Orge River (Nearby Paris, France). *Environ. Pollut.* **2011**, *159* (2), 391–397. https://doi.org/10.1016/j.envpol.2010.10.039.
(29) Wu, S. Chee.; Gschwend, P. M. Sorption Kinetics of Hydrophobic Organic Compounds to Natural Sediments and Soils. *Environ. Sci. Technol.* **1986**, *20* (7), 717–725. https://doi.org/10.1021/es00149a011.
(30) Brusseau, M. L. Transport of Reactive Contaminants in Heterogeneous Porous-Media. *Rev Geophys* **1994**, *32* (3), 285–313. https://doi.org/10.1029/94RG00624.
(31) Luthy, R. G.; Aiken, G. R.; Brusseau, M. L.; Cunningham, S. D.; Gschwend, P. M.; Pignatello, J. J.; Reinhard, M.; Traina, S. J.; Weber, W. J.; Westall, J. C. Sequestration of Hydrophobic Organic Contaminants by Geosorbents. *Env. Sci Technol* **1997**, *31* (12), 3341–3347.
(32) Pignatello, J. J.; Xing, B. Mechanisms of Slow Sorption of Organic Chemicals to Natural Particles. *Environ. Sci. Technol.* **1996**, *30* (1), 1–11. https://doi.org/10.1021/es940683g.

(33) Brusseau, M. L. Transport of Rate-Limited Sorbing Solutes in Heterogeneous Porous-Media - Application of a One-Dimensional Multifactor Nonideality Model to Field Data. *Water Resour Res* **1992**, *28* (9), 2485–2497. https://doi.org/10.1029/92WR00907.
(34) Pickens, J. F.; Jackson, R. E.; Inch, K. J.; Merritt, W. F. Measurement of Distribution Coefficients Using a Radial Injection Dual-Tracer Test. *Water Resour. Res.* **1981**, *17* (3), 529–544. https://doi.org/10.1029/WR017i003p00529.
(35) Brusseau, M. L.; Rao, P. S. C. The Influence of Sorbate-Organic Matter Interactions on Sorption Nonequilibrium. *Chemosphere* **1989**, *18* (9–10), 1691–1706. https://doi.org/10.1016/0045-6535(89)90453-0.
(36) Brusseau, M. L.; Rao, P. S. C. Influence of Sorbate Structure on Nonequilibrium Sorption of Organic Compounds. *Environ. Sci. Technol.* **1991**, *25* (8), 1501–1506. https://doi.org/10.1021/es00020a022.
(37) van Amerongen, G. J. Diffusion in Elastomers. *Rubber Chem. Technol.* **1964**, *37* (5), 1065–1152. https://doi.org/10.5254/1.3540396.
(38) Brusseau, M. L.; Jessup, R. E.; Rao, P. S. C. Nonequilibrium Sorption of Organic Chemicals: Elucidation of Rate-Limiting Processes. *Environ. Sci. Technol.* **1991**, *25* (1), 134–142. https://doi.org/10.1021/es00013a015.
(39) Brusseau, M. L.; Rao, P. S. C.; Jessup, R. E.; Davidson, J. M. Flow Interruption: A Method for Investigating Sorption Nonequilibrium. *J. Contam. Hydrol.* **1989**, *4* (3), 223–240. https://doi.org/10.1016/0169-7722(89)90010-7.
(40) Pennell, K. D.; Abriola, L. M.; Weber, W. J. Surfactant-Enhanced Solubilization of Residual Dodecane in Soil Columns .1. Experimental Investigation. *Env. Sci Technol* **1993**, *27* (12), 2332–2340. https://doi.org/10.1021/es00048a005.
(41) Taylor, T. P.; Pennell, K. D.; Abriola, L. M.; Dane, J. H. Surfactant Enhanced Recovery of Tetrachloroethylene from a Porous Medium Containing Low Permeability Lenses - 1. Experimental Studies. *J Contam Hydrol* **2001**, *48* (3–4), 325–350.
(42) Das, B. S.; Lee, L. S.; Rao, P. S. C.; Hultgren, R. P. Sorption and Degradation of Steroid Hormones in Soils during Transport: Column Studies and Model Evaluation. *Env. Sci Technol* **2004**, *38* (5), 1460–1470. https://doi.org/10.1021/es034898e.
(43) Fesch, C.; Simon, W.; Haderlein, S. B.; Reichert, P.; Schwarzenbach, R. P. Nonlinear Sorption and Nonequilibrium Solute Transport in Aggregated Porous Media: Experiments, Process Identification and Modeling. *J Contam Hydrol* **1998**, *31* (3–4), 373–407. https://doi.org/10.1016/s0169-7722(97)00078-8.
(44) Smits, K. M.; Sakaki, T.; Limsuwat, A.; Illangasekare, T. H. Thermal Conductivity of Sands under Varying Moisture and Porosity in Drainage-Wetting Cycles. *Vadose Zone J* **2009**, *9* (1), 172–180. https://doi.org/10.2136/vzj2009.0095.
(45) Pennell, K. D. Specific Surface Area☆. In *Reference Module in Earth Systems and Environmental Sciences*; Elsevier, 2016. https://doi.org/10.1016/B978-0-12-409548-9.09583-X.
(46) Goltz, M. N.; Roberts, P. V. Using the Method of Moments to Analyze Three-Dimensional Diffusion-Limited Solute Transport from Temporal and Spatial Perspectives. *Water Resour. Res.* **1987**, *23* (8), 1575–1585. https://doi.org/10.1029/WR023i008p01575.
(47) Higgins, C. P.; Field, J. A.; Criddle, C. S.; Luthy, R. G. Quantitative Determination of Perfluorochemicals in Sediments and Domestic Sludge. *Env. Sci Technol* **2005**, *39* (11), 3946–3956. https://doi.org/10.1021/es048245p.
(48) Schwarzenbach, R. P.; Gschwend, P. M.; Imboden, D. M. *Environmental Organic Chemistry, 2nd Edition*; Wiley-Interscience, 2003.

(49) Van Genuchten, M. T. *Determining Transport Parameters from Solute Displacement Experiments*; 118; U.S. Department of Agriculture: Riverside, CA, 1980.
(50) Simunek, J.; Sejna, M.; Saito, H.; Sakai, M.; Van Genuchten, M.T. *The HYDRUS-1D Software Package for Simulating the One-Dimensional Movement of Water, Heat, and Multiple Solutes in Variably-Saturated Media*; Department of Environmental Sciences University of California Riverside: Riverside, CA, 2013.
(51) van Genuchten, M. Th.; Wagenet, R. J. Two-Site/Two-Region Models for Pesticide Transport and Degradation: Theoretical Development and Analytical Solutions. *Soil Sci. Soc. Am. J.* **1989**, *53* (5), 1303. https://doi.org/10.2136/sssaj1989.03615995005300050001x.
(52) Li, Y.; Oliver, D. P.; Kookana, R. S. A Critical Analysis of Published Data to Discern the Role of Soil and Sediment Properties in Determining Sorption of per and Polyfluoroalkyl Substances (PFASs). *Sci. Total Environ.* **2018**, *628–629*, 110–120. https://doi.org/10.1016/j.scitotenv.2018.01.167.
(53) Zaggia, A.; Conte, L.; Falletti, L.; Fant, M.; Chiorboli, A. Use of Strong Anion Exchange Resins for the Removal of Perfluoroalkylated Substances from Contaminated Drinking Water in Batch and Continuous Pilot Plants. *Water Res.* **2016**, *91*, 137–146. https://doi.org/10.1016/j.watres.2015.12.039.
(54) McCleaf, P.; Englund, S.; Östlund, A.; Lindegren, K.; Wiberg, K.; Ahrens, L. Removal Efficiency of Multiple Poly- and Perfluoroalkyl Substances (PFASs) in Drinking Water Using Granular Activated Carbon (GAC) and Anion Exchange (AE) Column Tests. *Water Res.* **2017**, *120*, 77–87. https://doi.org/10.1016/j.watres.2017.04.057.
(55) Shinoda, K.; Hato, M.; Hayashi, T. Physicochemical Properties of Aqueous Solutions of Fluorinated Surfactants. *J. Phys. Chem.* **1972**, *76* (6), 909–914. https://doi.org/10.1021/j100650a021.
(56) Bernett, M. K.; Zisman, W. A. Wetting of Low-Energy Solids by Aqueous Solutions of Highly Fluorinated Acids and Salts. *J. Phys. Chem.* **1959**, *63* (11), 1911–1916. https://doi.org/10.1021/j150581a028.
(57) Brusseau, M. L.; Reid, M. E. Nonequilibrium Sorption of Organic Chemicals by Low Organic-Carbon Aquifer Materials. *Chemosphere* **1991**, *22* (3–4), 341–350. https://doi.org/10.1016/0045-6535(91)90322-5.
(58) Brusseau, M. L.; Jessup, R. E.; Rao, P. S. C. Nonequilibrium Sorption of Organic Chemicals: Elucidation of Rate-Limiting Processes. *Environ. Sci. Technol.* **1991**, *25* (1), 134–142. https://doi.org/10.1021/es00013a015.
(59) Higgins, C. P.; Luthy, R. G. Modeling Sorption of Anionic Surfactants onto Sediment Materials: An a Priori Approach for Perfluoroalkyl Surfactants and Linear Alkylbenzene Sulfonates. *Environ. Sci. Technol.* **2007**, *41* (9), 3254–3261. https://doi.org/10.1021/es062449j.
(60) Brusseau, M. L.; Larsen, T.; Christensen, T. H. Rate-Limited Sorption and Nonequilibrium Transport of Organic Chemicals in Low Organic Carbon Aquifer Materials. *Water Resour. Res.* **1991**, *27* (6), 1137–1145. https://doi.org/10.1029/91WR00503.
(61) Lee, L. S.; Rao, P. S. C.; Brusseau, M. L. Nonequilibrium Sorption and Transport of Neutral and Ionized Chlorophenols. *Environ. Sci. Technol.* **1991**, *25* (4), 722–729. https://doi.org/10.1021/es00016a018.
(62) Brusseau, M. L. Assessing the Potential Contributions of Additional Retention Processes to PFAS Retardation in the Subsurface. *Sci. Total Environ.* **2018**, *613–614*, 176–185. https://doi.org/10.1016/j.scitotenv.2017.09.065.

(63) Harding-Marjanovic, K. C.; Houtz, E. F.; Yi, S.; Field, J. A.; Sedlak, D. L.; Alvarez-Cohen, L. Aerobic Biotransformation of Fluorotelomer Thioether Amido Sulfonate (Lodyne) in AFFF-Amended Microcosms. *Environ. Sci. Technol.* **2015**, *49* (13), 7666–7674. https://doi.org/10.1021/acs.est.5b01219.
(64) Mejia Avendaño, S.; Liu, J. Production of PFOS from Aerobic Soil Biotransformation of Two Perfluoroalkyl Sulfonamide Derivatives. *Chemosphere* **2015**, *119*, 1084–1090. https://doi.org/10.1016/j.chemosphere.2014.09.059.